

GLOBAL TELECONNECTIONS ASSOCIATED WITH
INDIAN MONSOON AND ENSO

Tetsuzo Yasunari
Institute of Geoscience, University of Tsukuba,
Tsukuba, Ibaraki 305,
Japan

INTRODUCTION

Our previous studies (Yasunari, 1987a, b) shows that ENSO involves the global circulation changes through the evolution of the entire ENSO cycle. In the tropics, the eastward propagation of wind field anomalies from the Indian Ocean toward the eastern Pacific is noticeable (Yasunari, 1985). The northern middle and high latitudes, the distinct circulation anomalies are noted over the north Pacific and Eurasia during the intermediate stage from anti El Nino to El Nino (and vice versa). Particularly, the circulation anomalies over Eurasia are followed by the low-latitude anomalies over India/Indian Ocean, which in turn seem to be coupled with the eastward propagation of circulation anomalies along the equator. That is, the atmospheric processes over Eurasia through the Indian Ocean seem to have a key role on the mechanism of ENSO cycle.

The current study attempt to solve this problem. Special attention will be paid to the role of Indian summer monsoon on the interactions between the northern higher latitudes and the entire tropics with the interannual time scales.

DOMINANT MODE OF GLOBAL CIRCULATION

Fig. 1 shows the dominant mode of global circulation ($70^{\circ}\text{N} - 30^{\circ}\text{S}$) anomalies, deduced by applying the EOF analysis on the seasonal mean streamfunction anomalies at 200 mb. This mode occupies 38.3 % of the total interannual variances. The spatial pattern (Fig. 1(a)) correspond well to the anomalous circulation associated with the typical El Nino/ anti El Nino overturnings (Yasunari, 1987a). However, the time coefficients (Fig. 1(b)) suggest that the year to year Indian monsoon activity is also strongly associated with the oscillation of this mode. That is, the strong (weak) monsoon years correspond well to the ascending (descending) phase in the fluctuation of time coefficients, while the extreme values correspond to the El Nino/anti El Nino phases. In other words, it seems that ENSO is a manifestation of the extremely amplified phase of this mode which is fundamentally coupled with the Indian or Asian summer monsoon activity.

INDIAN MONSOON AND ENSO

Since Sir Gilbert Walker, many studies have already been made on the statistical relationship between Indian monsoon and ENSO. Some studies attempted to predict the Indian monsoon rainfall amount by using some ENSO related parameters such as SOI, SST and wind field in the equatorial Pacific (Shuka and Paolino, 1985; Nicholls, 1984 etc.). However, as has been suggested from Fig. 1, the Indian monsoon seems to play an important role on the formation of favourable condition for the initiation and termination of ENSO event over the Pacific. Very recently, we have presented some ample evidences that Indian summer monsoon activity has a great effect on the formation of heat content anomalies of the tropical western Pacific in the succeeding winter seasons (Yasunari, 1988). Fig. 2, for example, shows the lag correlations between the Indian monsoon rainfall and the SST anomalies in the equatorial western and eastern Pacific. It is noteworthy that the extreme values of correlation appear in the winter which follows the reference Indian summer monsoon season both in the western and eastern Pacific. Particularly in the western Pacific, the correlation is very high. That is, the piling up of warm water during the northern fall and winter, which has recently been noted as an important preconditioning of ENSO event in the eastern Pacific (e.g., White et al., 1987), is highly correlated with the strong Indian monsoon in the preceding summer.

TELECONNECTIONS ASSOCIATED WITH MONSOON AND ENSO

To deduce the seasonal-scale dominant teleconnection patterns in the northern hemisphere, the varimax rotated principal component analysis was applied to 3-month moving averaged monthly mean 500 mb geopotential height anomalies of the northern grids of 30°N to 70°N for 40 years (1946-1985). Fig. 3 shows the spatial eigenvector patterns of the first 10 dominant modes. These objectively deduced teleconnection patterns are surprisingly well correspond to those subjectively deduced by Wallace and Gutzler (1981). For example, the 1st mode corresponds to North Atlantic Oscillation (NAO) pattern, the 2nd mode to PNA pattern, the 4th mode to EU pattern, the 5th mode to WP pattern and so on. However, several new patterns are also found, some of which seem to have close associations with Indian monsoon and ENSO as discussed later.

To examine which teleconnection patterns are associated or not associated with Indian monsoon activity as well as with ENSO, 11 weak monsoon years are selected. Among these years, 6 ENSO years (1951, 1957, 1965, 1972, 1976, 1982) are also included. During the 40 years, there were actually no strong monsoon years with ENSO event. Fig. 4 shows the composite time coefficients of some significant modes for three years centered by the weak monsoon year ($Y(0)$), (a) with ENSO event and (b) without ENSO event.

It should be noted that both SOI and monsoon rainfall anomalies strongly suggest the nature of biennial cycle especially in the period of $Y(-1)$ through the beginning of $Y(+1)$ in the case with ENSO. There is also a remarkable difference in

SOI tendency from the winter of $Y(-1)/Y(0)$ to the summer of $Y(0)$ between the two cases. To examine the teleconnection patterns associated with this remarkable feature, we note the difference of dominant patterns during the winter of $Y(-1)/Y(0)$. During this season, positive coefficients of Eurasian (EU) pattern and negative coefficients of PNA-II pattern are commonly apparent in both cases. That is, negative height anomalies over Scandinavia through central Asia and positive anomalies to the east and west are dominant over Eurasia, while the pattern of positive anomalies over north Pacific and negative anomalies over northeast part of north America seems to be dominant over north American sector. These patterns may be associated with the following weak summer monsoons. Particularly in the case with ENSO, the amplitudes of these two patterns are large.

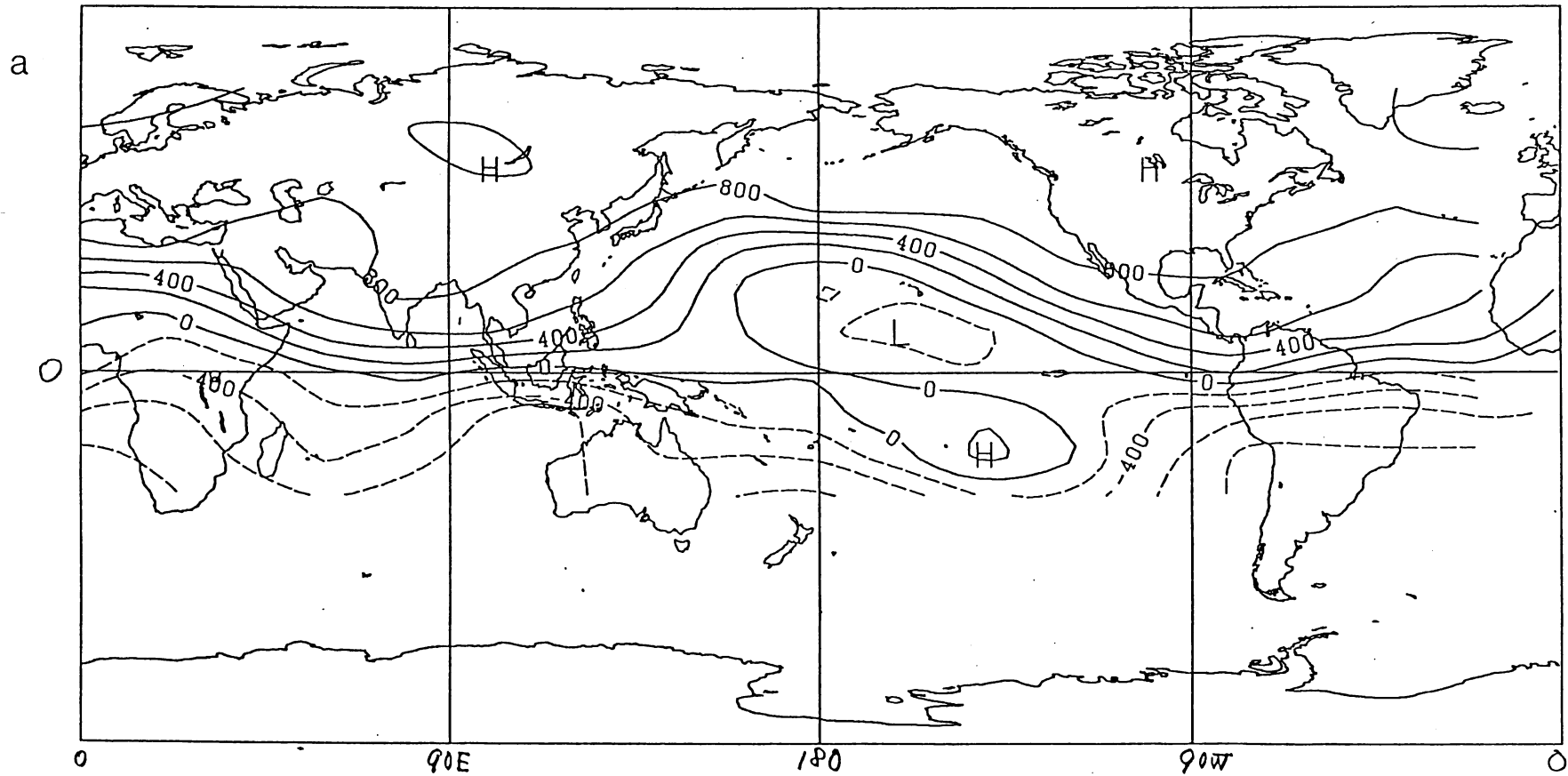
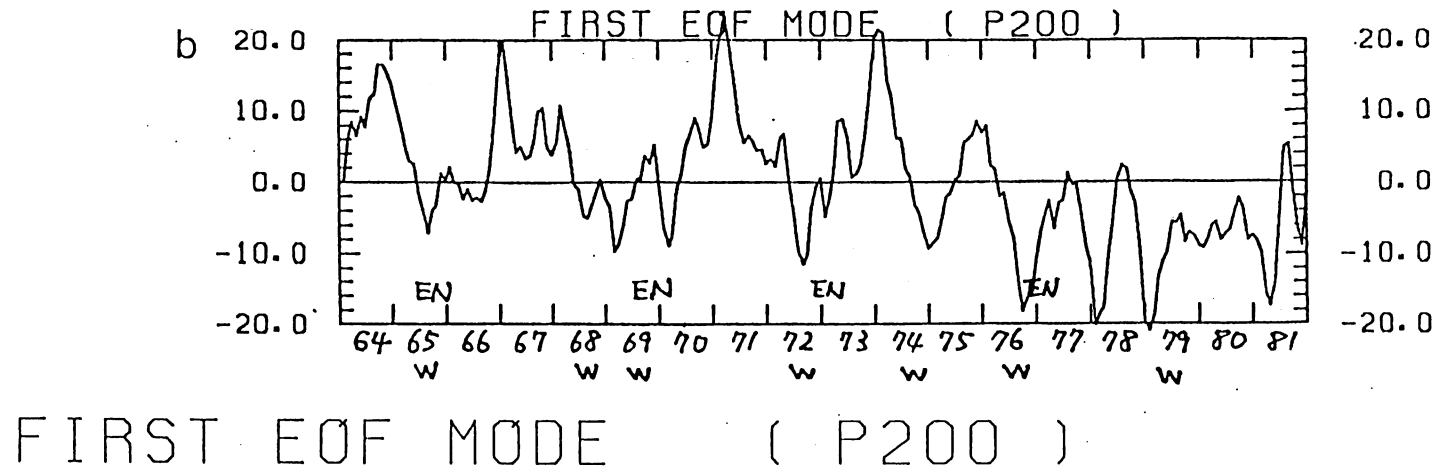
A distinct difference between the two cases exists in the phase of North Atlantic Oscillation (NAO) pattern, as shown in the sign of time coefficients. In the case with ENSO the coefficients show large negative values, which implies the phase of NAO with the north/negative and the south/positive height anomalies. In the case without ENSO just the opposite condition appears over the north Atlantic sector. Some previous arguments (e.g., Barnett, 1985) suggest the independency or orthogonality in time variation between SO and NAO. However, this may not deny the possibility of the phase locking of NAO with some particular phase of the ENSO cycle. The atmospheric circulation anomalies composited for each phase of the ENSO cycle (Yasunari, 1987b) also suggest the time-lagged association between the SO and the NAO.

CONCLUSIONS

These results suggest that there is fundamentally a quasi-biennial oscillation in the Indian summer monsoon activity, which seems to be coupled with some particular teleconnection patterns in the 500 mb height anomalies over Eurasian continent and north Pacific/north American sector. However, whether the ENSO event occurs or no, seems to depend, as far as the northern hemisphere is concerned, on another factor, i.e., the phase of the NAO. During the preceding winter of ENSO year, the coupling of the teleconnection patterns associated with the preceding strong Indian monsoon and the NAO may produce the anomalous circulation pattern over Eurasia through the Indian Ocean, that is favorable for triggering the ENSO event over the equatorial Pacific. Further detailed analysis is being undertaken and will be reported elsewhere.

References

- Barnett, T., 1985: Variations near-global sea level pressure. *J.Atmos.Sci.*, 42, 478-501.
- Nicholls, N., 1984: Predicting Indian monsoon rainfall from sea-surface temperature in the Indonesia-north Australia area. *Nature*, 307, 576-577.
- Shukla, J. and D.A. Paolino, 1983: the Southern Oscillation and long-range forecasting of the summer monsoon rainfall over India. *Mon.Wea.Rev.*, 111, 1830-1837.
- Wallace, J.M. and D.S. Gutzler, 1981: Teleconnections in the geopotential height field during the northern hemisphere winter. *Mon.Wea.Rev.*, 109, 784-812.
- White, W.B., S.E. Pazan and M. Inoue, 1987: Hindcast/forecast of ENSO events based upon the redistribution of observed and model heat content in the western Pacific. *J.Phys.Oceanogr.*, 17, 264-280.
- Yasunari, T., 1985: Zonally propagating modes of the global east-west circulation associated with the Southern Oscillation. *J.Met.Soc.Japan*, 63, 1013-1029.
- , 1987a: Global structure of the El Nino/Southern Oscillation. Part I. El Nino composites. *J.Met.Soc.Japan*, 65, 67-80.
- , 1987b: Global structure of the El Nino/Southern Oscillation. Part II. Time evolution. *J.Met.Soc.Japan*, 65, 81-102.
- , 1988: Impact of Indian monsoon on the ocean mixed layer temperature in the tropical Pacific. To be submitted.



CONTOUR FROM $-0.80000E-01$ TO 0.10000 . CONTOUR INTERVAL OF $0.20000E-01$ PT (3,3) = $-0.47000E-01$ LABELS SCALED BY 10000.

Fig. 1 First eigenvectors for streamfunction anomalies at 200 mb (38.3%) (a) and its time coefficients (b). In (b) EN denotes El Niño year, and W denotes weak summer monsoon year.

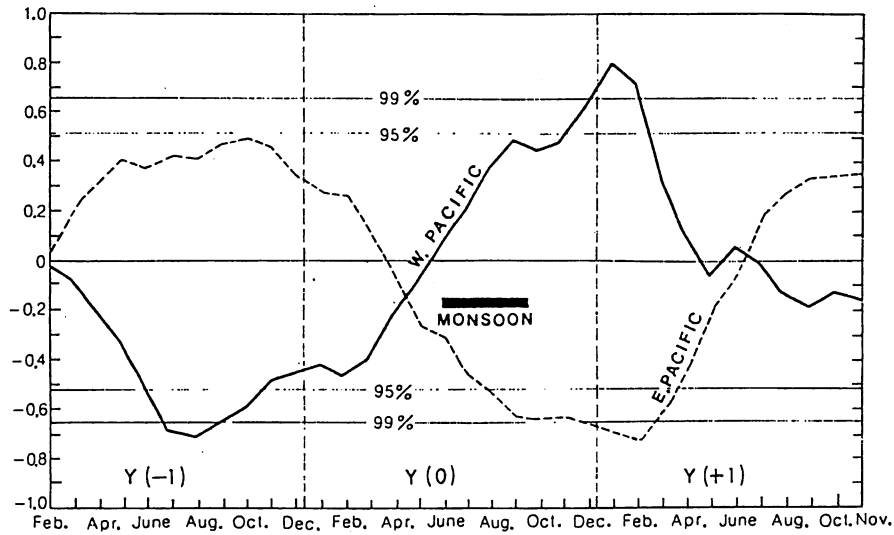
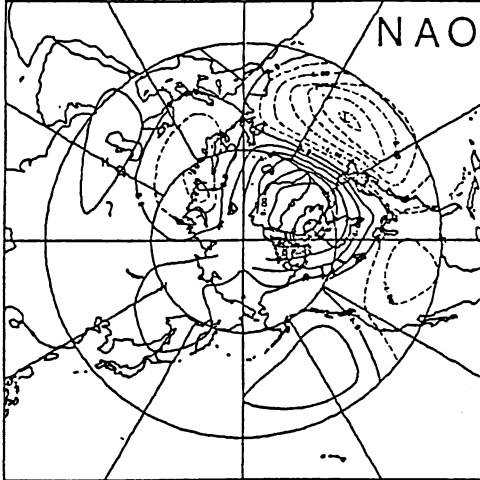
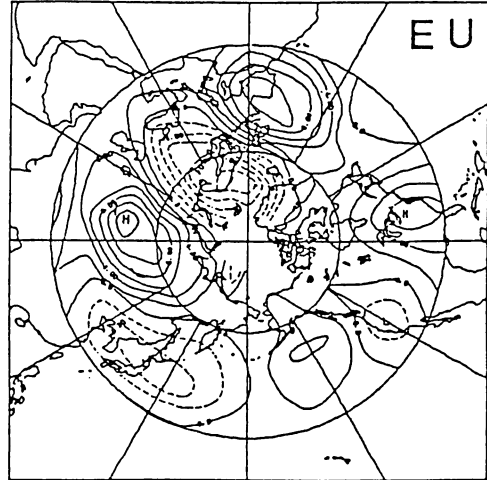


Fig. 2 Lag-correlations between Indian monsoon rainfall and sea surface temperature in the western Pacific ($0^{\circ} - 8^{\circ}$ N, 130° E - 150° E) and the eastern Pacific ($0^{\circ} - 8^{\circ}$ N, 170° W - 150° W). Reference monsoon is shown with thick black bar. Y(0) denotes the year of reference monsoon and Y(-1) (Y(+1)) denotes the year before (after) the reference monsoon year. (Yasunari, 1988)

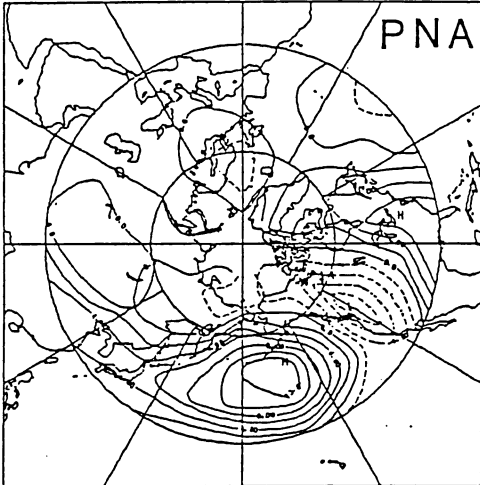
VARIMAX VCT OF 3-MONTH RUNN MODE COMP. 1



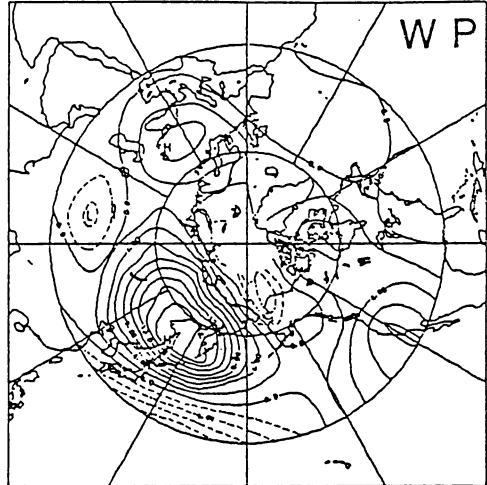
VARIMAX VCT OF 3-MONTH RUNN MODE COMP. 4



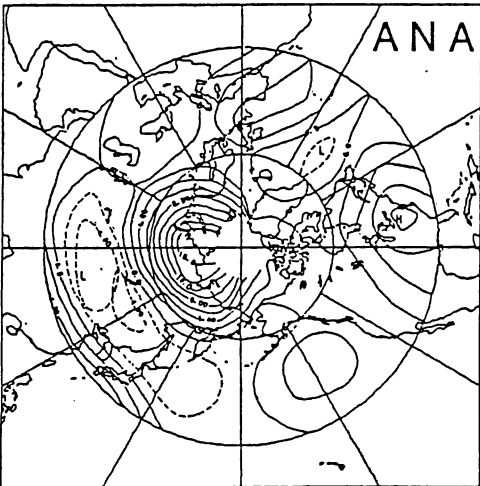
VARIMAX VCT OF 3-MONTH RUNN MODE COMP. 2



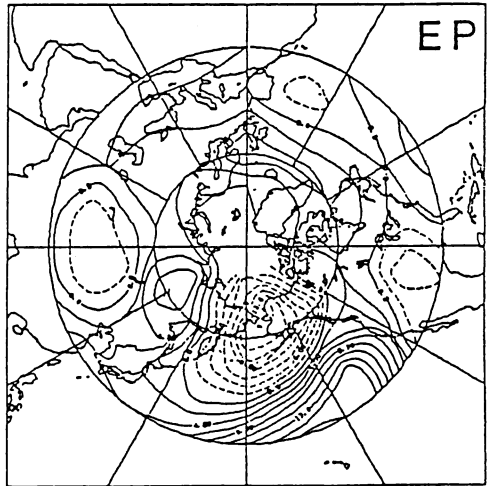
VARIMAX VCT OF 3-MONTH RUNN MODE COMP. 5



VARIMAX VCT OF 3-MONTH RUNN MODE COMP. 3



VARIMAX VCT OF 3-MONTH RUNN MODE COMP. 6



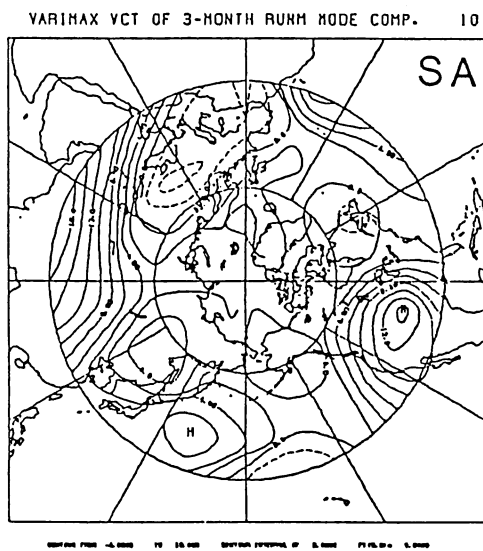
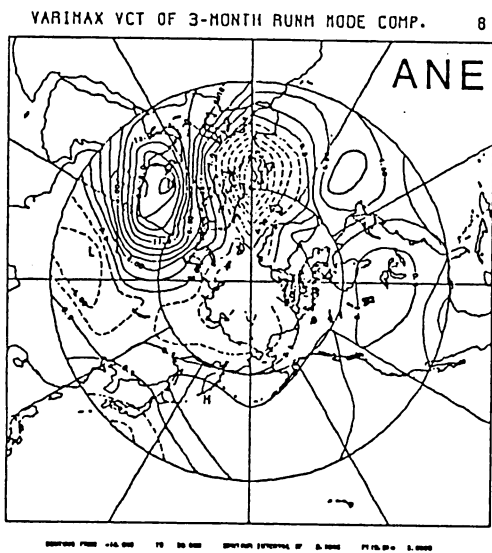
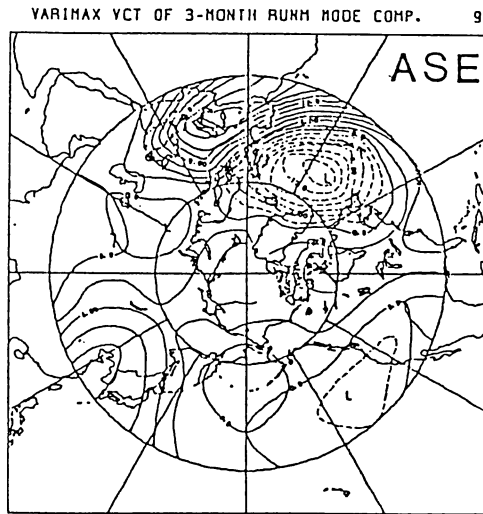
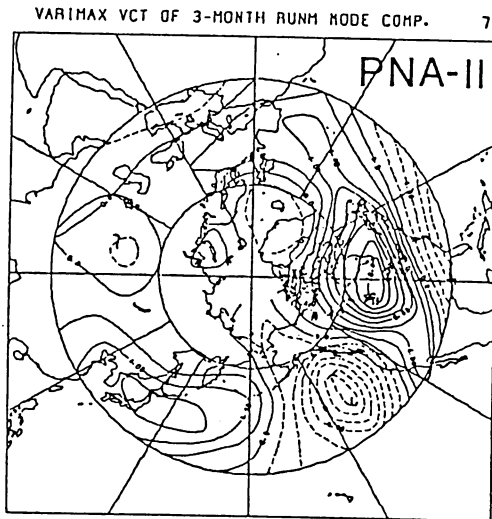


Fig. 3 10 principal modes of varimax-rotated eigenvectors for smoothed monthly 500 mb height anomalies. Negative values are shown with dashed lines.

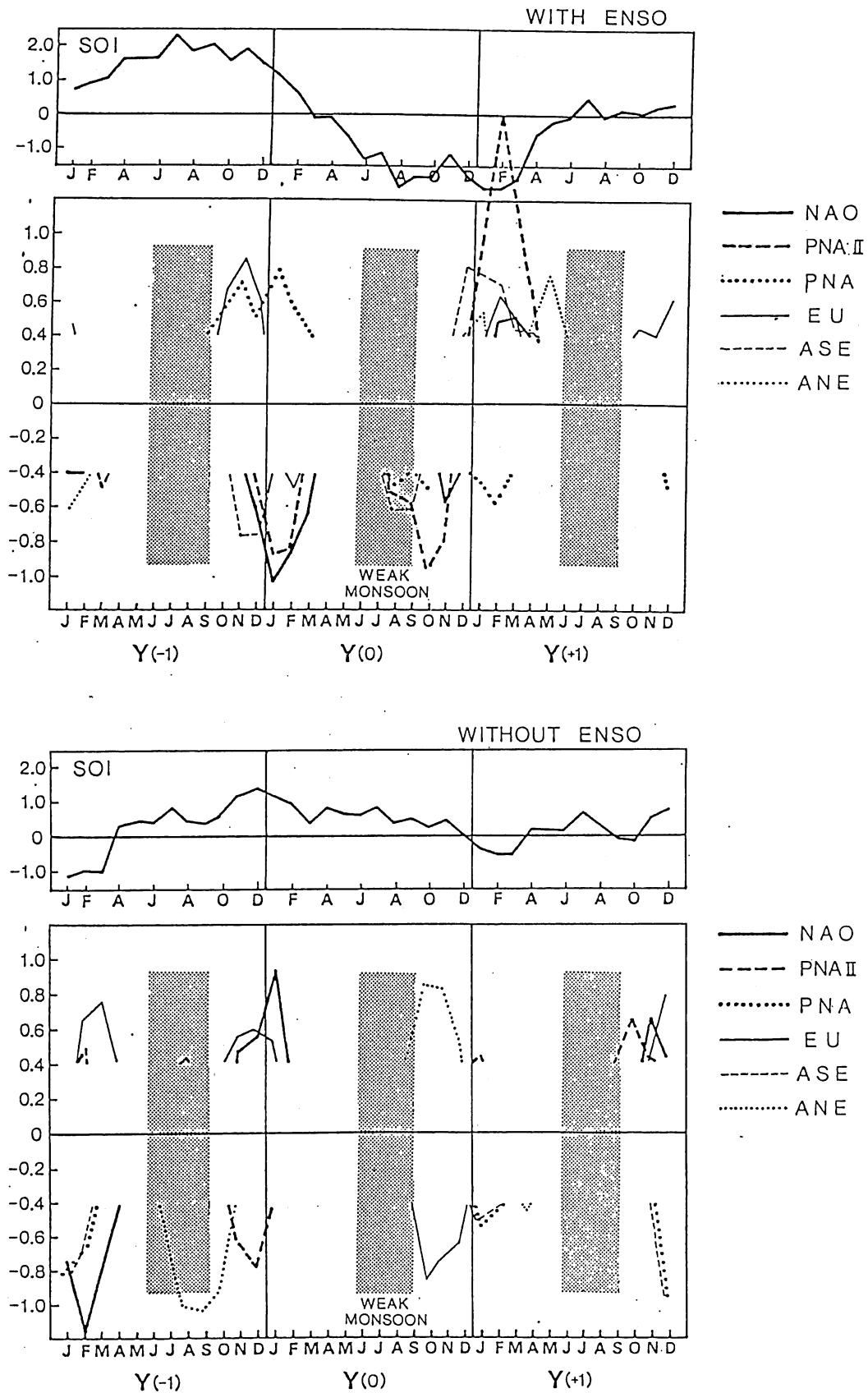


Fig. 4 Composite time sequences of time coefficients of some teleconnection patterns in reference to weak monsoon years (Y(0)) (a) with ENSO events and (b) without ENSO events. Coefficients whose absolute values are less than 0.4 are not indicated. Composite SOI anomalies are also shown in the upper part of each diagram. Indian monsoon seasons are shown with hatched areas.